Base-free palladium-catalyzed borylation of enol carboxylates and further reactivity toward deboronation and cross-coupling

Gregory Gaube, Douglas L. Miller, Rowan A. McCallum, Nahiane Pipaón Fernández, and David C. Leitch

2025

Faculty of Science

Faculty Publications

© 2025 The Authors. This is an open access article distributed under the terms of the Creative Commons license CC BY-NC-ND: http://creativecommons.org/licenses/by-nc-nd/4.0/.

Original citation:
Gaube, G., Miller, D. L., McCallum, R. A., Fernández, N. P., & Leitch, D. C. (2025). Base-free palladium-catalyzed borylation of enol carboxylates and further reactivity toward deboronation and cross-coupling. *Tetrahedron*, *182*, 134682. https://doi.org/10.1016/j.tet.2025.134682

Downloaded from UVicSpace Research & Learning Repository

dspace.library.uvic.ca

University of Victoria | Libraries

Tetrahedron 182 (2025) 134682

Contents lists available at ScienceDirect

Tetrahedron

journal homepage: www.elsevier.com/locate/tet

Base-free palladium-catalyzed borylation of enol carboxylates and further reactivity toward deboronation and cross-coupling

Gregory Gaube, Douglas L. Miller, Rowan A. McCallum, Nahiane Pipaón Fernández, David C. Leitch *

Department of Chemistry, University of Victoria, Victoria, Canada

ARTICLE INFO

Keywords:
Borylation
Cross-coupling
C–O activation
Palladium catalysis
Deoxygenation
High-throughput experimentation

ABSTRACT

A series of base-free Pd-catalyzed borylation procedures are reported for a number of alkenyl carboxylates, with pivalates generally outperforming their acetate counterparts. High-throughput experimentation was used to discover and optimize these reactions using *in situ* generated catalyst systems. Mechanistic studies identified C–O oxidative addition to Pd(0) as the turnover-limiting step, with a variety of rates observed depending on substrate structure. One exemplar oxidative addition complex was isolated and fully characterized, including by X-ray crystallography. This complex undergoes rapid and complete reaction with excess B_2Pin_2 at room temperature, confirming that no exogeneous base is required for transmetallation with the Pd(II) pivalate intermediate. Notably, gamma-lactone and lactam substrates lead to unstable alkenyl pinacol boronates, which undergo protodeboronation under acidic and basic aqueous conditions. Optimization of this protodeboronation resulted in a mild, two-step reduction of the C–O bond, achieving net-deoxygenation while leaving the alkene intact. In contrast, use of an alternative tetraalkoxydiboron source – B_2EPin_2 – was successful in catalysis, and offered improved stability of the resulting organoboron species. This enables further reactivity, such as cross-coupling, without competing protodeboronation.

1. Introduction

Installation of boron-based functional groups is a valuable methodology, particularly in the context of metal-catalyzed cross-coupling [1–7]. Although numerous reactions utilize organoboron intermediates, Suzuki-Miyaura coupling is the most widespread, as it remains one of the most reliable methods for forming C–C bonds [8–16]. Accordingly, a plethora of methods to install a suitable boron-based unit are known [17–21]. Since seminal work from Miyaura [22], Pd-catalyzed borylation of organohalides and *pseudo* halides (such as triflates) is often used achieve this [23,24], typically with a tetraalkoxydiboron source (such as B_2Pin_2 or an alternative) [25] and a weak base (such as KOAc or other carboxylate bases) [26–28] to complete the catalytic cycle. Importantly, the vast majority of these reactions rely on the aforementioned halide or triflate electrophiles to accomplish this transformation.

Two ways to improve Pd-catalyzed borylation are to utilize alternative, non-halide electrophiles, and to eliminate the need for insoluble inorganic bases. For the former, simple oxygen based leaving groups such as alkoxyl or carboxyl are advantageous from an accessibility/installation standpoint [29,30]; however, the required C–O activation is kinetically difficult [31], limiting the reported examples of C–O borylation to select systems based on Rh [32–34], Ni [35–39], and Fe (Fig. 1a) [40,41]. For the latter, conditions that use homogeneous bases, or no base at all, would greatly improve reliability and scalability of these reactions, an important consideration in pharmaceutical process chemistry [42–44].

In both cases, carboxylate leaving groups offer several advantages [45]. They are easily installed by simple acylation, and the intermediacy of a Pd(II) carboxylate after C–O oxidative addition means that exogenous base should not be required. However, since carboxylates contain two C–O bonds for Pd(0) to react with, an additional selectivity hurdle needs to be overcome. Accordingly, to the best of our knowledge there is a single, Rh-based catalytic system able effect borylation with carboxylate-based electrophiles [32].

While the Newman group has selectively activated the acyl C–O bond using Pd catalysis [31], a 2020 publication by our lab has shown that Pd (0) can selectively insert into the desired aryl/alkenyl C–O bond in heteroaryl and alkenyl carboxylates [46]. This was then applied to

* Corresponding author. Department of Chemistry, University of Victoria, 3800 Finnerty Rd., Victoria, BC, V8P 5C2, Canada.
E-mail address: dcleitch@uvic.ca (D.C. Leitch).

https://doi.org/10.1016/j.tet.2025.134682
Received 14 February 2025; Received in revised form 22 April 2025; Accepted 23 April 2025
Available online 3 May 2025
0040-4020/© 2025 The Authors. Published by Elsevier Ltd. This is an open access article under the CC BY-NC-ND license (http://creativecommons.org/licenses/by-nc-nd/4.0/).

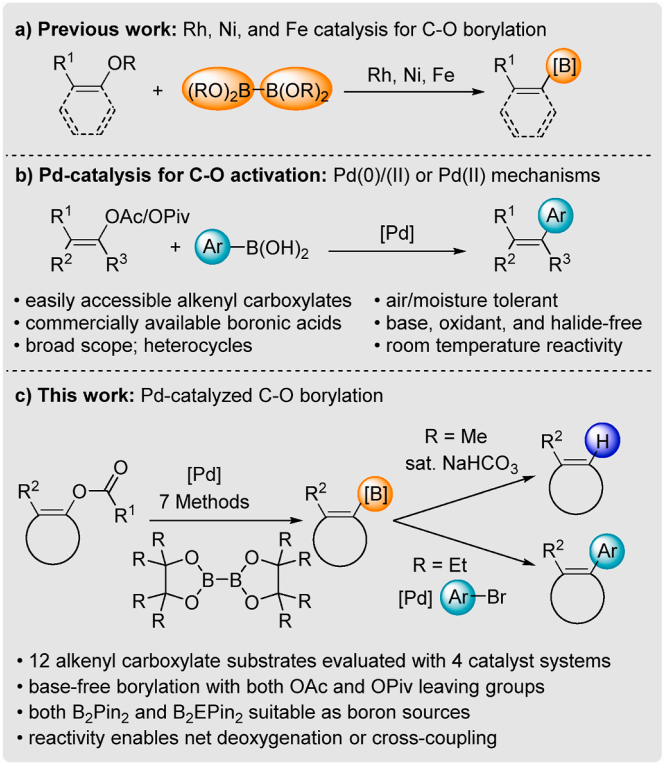

Fig. 1. **a**) Prior catalytic strategies for C–O borylation; **b**) C–O activation in C–C bond formation with arylboronic acids; **c**) an evaluation of catalytic systems for borylation involving C–O activation, including comparable reactivity of two systems with both BPin and BEPin synthetic handles.

Pd-catalyzed reactions of alkenyl carboxylates and phenyl boronic acids without the use of a base (Fig. 1b) [47]. We have since expanded this reactivity to tandem C–O/C–H activation for base-free direct alkenylation [48].

Herein, we expand on a prior communication [49] regarding Pd-catalyzed Miyaura borylation of alkenyl carboxylates. We have developed several Pd-catalyzed borylation procedures (Fig. 1c), including using an air-stable Pd precatalyst (^{DMP}DAB–Pd–MAH) recently developed within our group [50]. We have also investigated the protodeboronation of alkenyl boronate esters derived from γ-lactones and γ-lactams. Using the standard BPin group, protodeboronation is readily achieved using biphasic hydrolysis under mildly basic conditions. Optimization of this deboronation results in a net reductive deoxygenation of the precursor enols, using conditions that leave the C=C bond intact. In contrast, use of the recently reported B_2EPin_2 under our catalytic conditions gives stable organoboron compounds that can be used further [51].

2. Results and discussion

2.1. Borylation conditions for multiple substrate classes

Our prior work on Pd-catalyzed Suzuki-Miyaura coupling with alkenyl carboxylates yielded two viable catalytic systems, both of which operate base-free [47]. One *in situ* system with $Pd(OAc)_2$ and tris (*ortho*-methoxyphenyl)phosphine functioned open to air, at room temperature, and in the presence of water, potentially through a redox-neutral Pd(II)-based mechanism [52–54]. The other system involves a single component Pd(0) catalyst, $Pd(PCy_3)_2$, which functioned at higher temperatures, through a more typical Pd(0)/(II) mechanism [47]. To determine if additional Pd/ligand combinations would yield product in a base-free Miyaura borylation, we conducted a series of microscale high-throughput screening experiments against multiple classes of alkenyl carboxylate electrophiles (Fig. 2).

Our screening approach was two-pronged. First, dimedone-derived alkenyl acetate **1a** was reacted with B_2Pin_2 at elevated temperature with twenty *in situ* catalyst combinations involving four Pd precatalysts and five ligands. We explored two Pd(II) and two Pd(0) precatalysts, including ^{DMP}DAB-Pd-MAH [50], a precatalyst developed within our group. These precatalysts were assessed with five ligands: P(*o*-MeOPh)$_3$ and PCy_3 (both successful in the prior Suzuki-Miyaura coupling method) [47], as well as SPhos, dppf and XPhos. Control experiments without ligand resulted in little to no product formation (SI -Figure S1), and a further control experiment without Pd also yielded no product. Many combinations yielded product, but generally Pd(II) sources outperformed Pd(0) sources. $Pd(OAc)_2$ and SPhos was the best *in situ* combination (62 % solution yield), and was taken forward in further optimization. We also evaluated a single component Pd precatalyst $Pd(PCy_3)_2$ that also yielded comparable product formation (SI - Figure S1) [55].

The second round of screening aimed at identifying an *in situ* catalyst system for borylation of six γ-lactone and γ-lactam alkenyl pivalate substrates (**2b-2g**). The choice of pivalate as opposed to acetate was informed by further exploration of the dimedone-based system (*vide infra*). We opted to explore electronic effects by changing the *para* substituent on the phenyl ring at the α position. The aryl was either unsubstituted (-H) or substituted with an electron-withdrawing (-CF_3) or electron-donating (-OMe) group. The resulting 6 compounds were evaluated with the same twenty *in situ* combinations of Pd and ligands (Fig. 2). Many combinations facilitated borylation; however, in contrast to **1a**, the lactone and lactam substrates generally preferred Pd(0) over Pd(II) sources. Control experiments with no catalyst again yielded no borylated product. With respect to ligand effects, every Pd source when combined with PCy_3 facilitated borylation to some extent. Notably, lactone substrates (**2b-d**) have generally higher reactivity than their lactam counterparts (**2e-g**): XPhos and SPhos performed reasonably well with the former set, but were generally ineffective for the latter set. Taken holistically, these results reveal that the combination of ^{DMP}DAB-Pd-MAH and PCy_3 performed well among all six substrates, with solution yields of the organoboron products between 61 and 98 %.

Moving ahead, full factorial multivariate optimization was chosen to quickly obtain improved conditions for the $Pd(OAc)_2$/SPhos *in situ* system (Fig. 3). Three variables were chosen for evaluation: concentration of Pd, concentration of ligand, and concentration of B_2Pin_2. Notably, excess ligand (3 equiv. to Pd) reduced yield with both the 4 and 10 mol% $Pd(OAc)_2$ reactions. This is consistent with a monoligated Pd(0) species as the active catalyst. In all cases, increasing the B_2Pin_2 in the reaction mixture improved yields of **3a**, while only marginally increasing the conversion. Optimal conditions were found to be 0.2 M **1a**, 10 mol% Pd $(OAc)_2$, 15 mol% SPhos, and two equivalents of B_2Pin_2, giving 71 % solution yield, but only 89 % conversion.

While this result was satisfactory in yield, the high Pd loading (turnover number (TON) = 7) and incomplete conversion were concerning. Furthermore, increasing [**1a**] while maintaining constant [catalyst] did lead to higher TON (up to 18), but also led to diminished yields of **3a**, which we attribute to competitive decomposition of **1a**. To correct this, we evaluated the more sterically-hindered, electron-rich alkenyl pivalate derivate **2a** at a concentration of 0.8 M. This greatly improved the yield of **3a** (72 % solution yield), the mass balance, and the TON (29).

Full factorial multivariate optimization was also performed for substrates **2b-g** with the ^{DMP}DAB-Pd-MAH/PCy_3 *in situ* system. A simplified two factor, two level design, in catalyst loading and B_2Pin_2 equivalents was conducted (Fig. 4). The Pd:PCy_3 ratio was held steady at 1:2. We found that the best conditions are dependent on the motif. Consistent with initial screening, γ-lactams are less reactive, requiring both higher catalyst loading (5 mol%) and two equivalents of B_2Pin_2 (92–98 % solution yields) (Method **D**). In an effort to reduce B_2Pin_2, and therefore

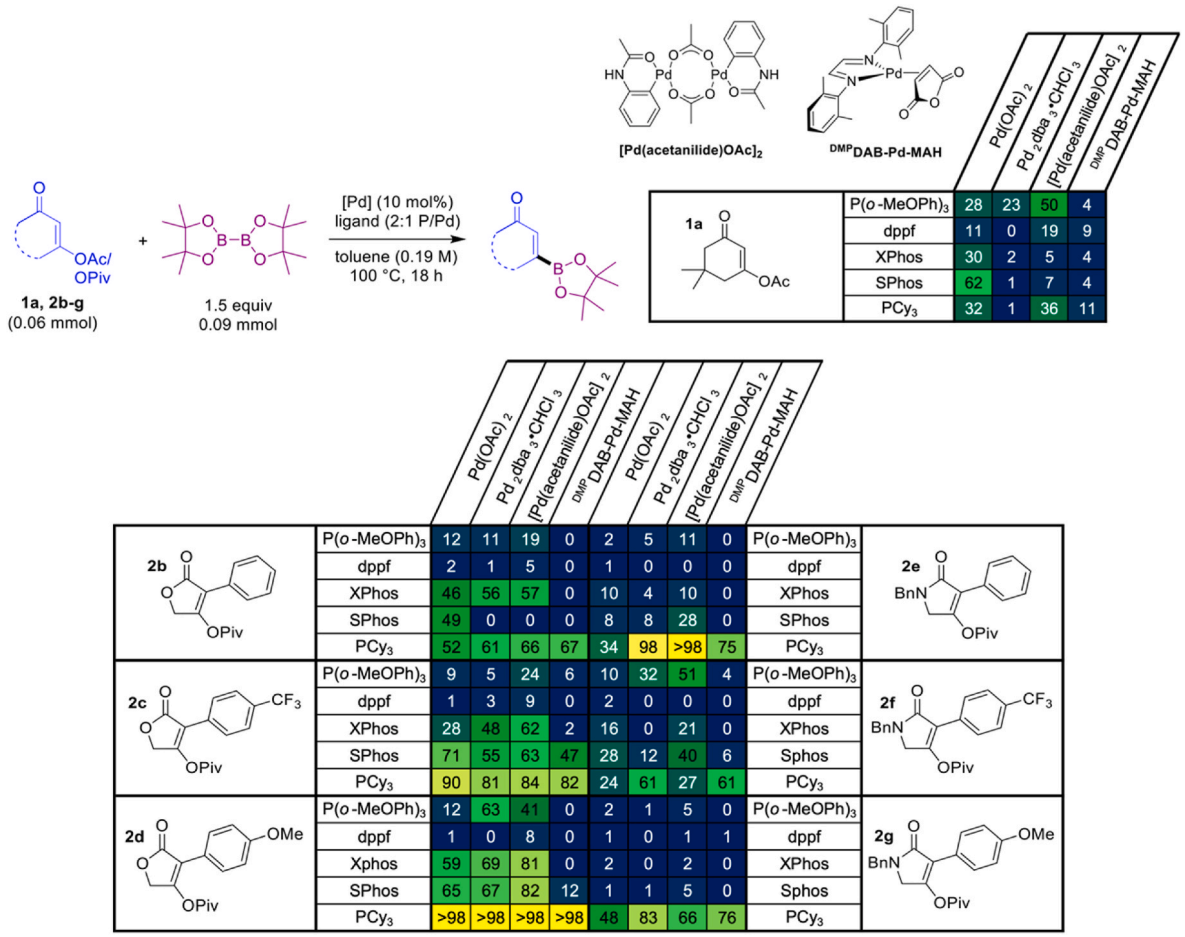

Fig. 2. Catalyst screening for the borylation of **1a**, **2b-2g**. Yield determined by ^{1}H NMR spectroscopy using 1,3,5-trimethoxybenzene internal standard.

downstream pinacol-containing impurities, an additional data point (5 mol% [Pd] and 1.6 equiv B_2Pin_2) was collected for **2e-g**; however, this resulted in reduced yield for **2f**. The γ-lactones **2b-d** had similar results with 2.0 mol% [Pd] and two equiv B_2Pin_2, and 3.5 mol% [Pd] and 1.6 equiv B_2Pin_2; the latter was denoted as Method **E** because excess B_2Pin_2 has been found to hamper purification in further steps [56].

After these two targeted optimizations, we wanted to evaluate the utility of these procedures against the two methods our group had used previously for C–O activation in Suzuki-Miyaura coupling. For this assessment, we prepared twelve alkenyl carboxylates, including six main motifs with both acetate and pivalate leaving groups. Specifically, these are the previously described dimedone-derived substrates (**1**/**2a**), the γ-lactones (**1**/**2b**) and γ-lactams (**1**/**2e**), along with cyclopentanone derived substrates (**1**/**2h**), coumarins (**1**/**2i**) and pyrones (**1**/**2j**). These substrates were subjected to six reaction conditions, with Methods **A**-**D** shown in Fig. 5 (two additional Methods **F** & **G** shown in SI - Figure S2). Method **A** was previously used in Pd(II) catalyzed C–O activation cross-coupling, Method **B** is the $Pd(OAc)_2$/SPhos system optimized for **1**/**2a**, Method **C** was previously used for Pd(0) catalyzed C–O activation cross-coupling, and Method **D** is the ^{DMP}DAB-Pd-MAH/PCy_3 system (5 mol% loading) optimized for **2e-2g**. Each of the alkenyl pinacol boronate compounds were characterized (NMR, HRMS) without purification, as attempts to use column chromatography or selective extractions led to product decomposition (*vide infra*) and/or pinacol-containing impurities remaining; this latter issue is a known problem when synthesizing BPin-containing molecules [1].

Overall, alkenyl pivalate substrates performed uniformly better than their alkenyl acetate counterparts, and no method proved optimal across all evaluated substrates. For the formation of **3a**, Method **B** proved to be best, which is consistent with our multivariate optimization; however, this method appears to be specific to the dimedone motif, as these conditions failed to borylate the similar cyclopentenone **1**/**2h**, and provided low yields for the other motifs. Method D proved to be best for the formation of **3b** and **3e** from the corresponding pivalates; however, Method **C** (which uses the same PCy_3 ligand) gave similar, albeit slightly lower yields with higher catalyst loading. Furthermore, while $Pd(PCy_3)_2$ is commercially available, its air sensitivity is a practical limitation; ^{DMP}DAB-Pd-MAH is air stable and readily substitutes its *N,N′*-bis(2,6-dimethylphenyl)-1,4-diazabutadiene (^{DMP}DAB) ligand for phosphine ligands [50]. For the formation of **3h** from the corresponding pivalate, Method **A** was best, which is again specific to this motif. Finally, formation of **3i** and **3j** was best using Method **C**. Given the success of PCy_3-based systems, we also evaluated $Pd(OAc)_2(PCy_3)_2$ as a single component Pd(II) source. This complex has been observed to reduce *in situ* to $Pd(PCy_3)_2$ in the presence of B_2Pin_2 [55]; however, this ultimately proved inferior to $Pd(PCy_3)_2$ (Methods **F** & **G**, SI - Figure S2).

As borylated compounds are usually targeted as synthetic intermediates, we chose to assess the newly formed alkenyl pinacol boronates in preparative scale Suzuki-Miyaura cross-coupling reactions. Enol pivalates **2a**, **b**, **e**, **h-j** were first borylated at a 1 mmol scale via the best Method from Fig. 5 (**2b** and **2e** borylated using Method **C**) to obtain the respective organoboron compounds **3a**, **b**, **e**, **h-j**. These were then subject to a typical (and unoptimized) Suzuki-Miyaura cross-coupling protocol, allowing the isolation of the arylated product **5a**, **h-j** in moderate yields (Fig. 6). However, coupling reactions with **3b** and **3e** resulted in low yields of the respective arylated products: coupling of **3b**

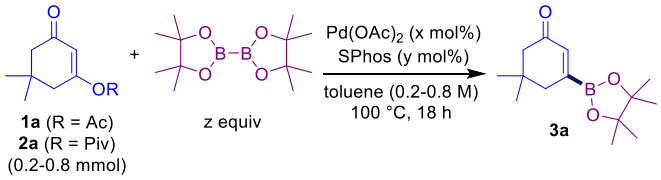

Substrate	[1] (M)	Pd(OAc)$_2$ loading (mol%)	SPhos equiv per Pd	B$_2$Pin$_2$ equiv	% Conv. *a*	% Yield **3a**	
1a	0.2	4.0	1.5	1.1	29	11	
				2.0	40	25	
			3.0	1.1	30	1	
				2.0	40	19	
		7.5	1.5	1.5	58	33	Centerpoint
		10.0	1.5	1.1	66	40	
				2.0	89	71	Maximum
			3.0	1.1	74	44	
				2.0	92	62	
1a	0.2	10.0	1.5	2.0	89	71	TON = 7
	0.4	5.0			>98	67	TON = 13
	0.6	3.3			>98	58	TON = 18
	0.8	2.5			>98	44	TON = 18
2a	0.8	2.5	1.5	2.0	>98	72	TON = 29

Fig. 3. Multivariate optimization of the borylation of **1a**. Conversion and yield determined by ^{1}H NMR spectroscopy using 1,3,5-trimethoxybenzene internal standard.

resulted in a negligible yield (<2 % isolated) and **4b** observed as the major product, while coupling of **3e** resulted as an inseparable mixture of arylated and deboronated products (49 % yield of a 3.33 : 1 mixture of **5e** and **4e**). In other words, the protodeboronated products (**4b** and **4e**) are observed as the major species in these reactions.

2.2. Mechanistic studies

The results in Fig. 5 generate several mechanistic questions. First among these is the reason for alkenyl pivalate substrates universally outperforming their acetate counterparts. Our initial hypothesis was that starting material decomposition is a significant issue with the acetate leaving group. We thought this would proceed either via direct hydrolysis (by adventitious water), or via competitive C_{acyl}–O oxidative addition to Pd(0) to generate an O-bound Pd(II) enolate. We previously observed this latter pathway for coumarin (**1i**) and pyrone (**1j**) acetates in stoichiometric oxidative addition experiments [46]. To test this hypothesis for other substrates, we subjected dimedone-derived alkenyl carboxylates **1a** (OAc) and **2a** (OPiv) to the Method **B** reaction conditions in the absence of B_2Pin_2, and analyzed the outcome by ^{1}H NMR spectroscopy. For **1a**, we observe an approximately 1:1 mixture of unreacted alkenyl acetate to a second species we assign as an enol isomer (**1a'**) generated via intramolecular acyl transfer (eq. (1)). Importantly, the corresponding alkenyl pivalate **2a** is largely unperturbed under analogous conditions. An analogous experiment comparing the

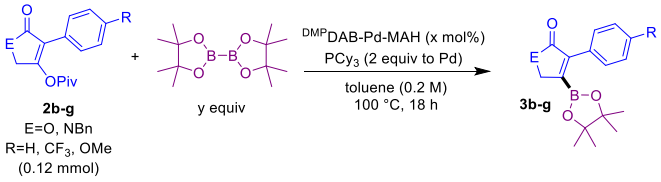

DMP DAB-Pd-MAH (mol%)	B$_2$Pin$_2$ equiv.	% Yield **3b**	% Yield **3c**	% Yield **3d**	% Yield **3e**	% Yield **3f**	% Yield **3g**
2	1.2	95	64	96	86	24	38
	2	>98	>98	95	97	33	73
3.5	1.6	>98	96	98	87	63	>98
5	1.2	>98	96	>98	81	91	>98
	1.6				>98	72	>98
	2	>98	95	97	>98	92	>98

Fig. 4. Full factorial optimization of the borylation of **2b-2g**. Yield was determined by ^{1}H NMR spectroscopy using 1,3,5-trimethoxybenzene internal standard. Grey cells indicate reactions not performed under these conditions.

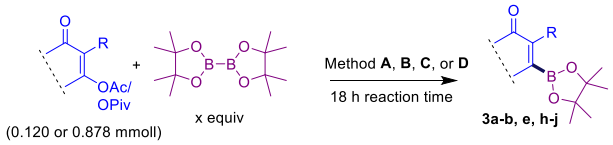

Method **A**: Pd(OAc)$_2$ (4 mol%) / P(*o*-OMePh)$_3$ (6 mol%), x = 1.1, acetone/water (10:1, 0.6 M), rt
Method **B**: Pd(OAc)$_2$ (2.5 mol%) / SPhos (3.8 mol%), x = 1.1, toluene (0.8 M), 100 °C
Method **C**: Pd(PCy$_3$)$_2$ (10 mol%), x = 1.1, toluene (0.2 M), 100 °C
Method **D**: DMPDAB-Pd-MAH (5 mol%) / PCy$_3$ (10 mol%), x = 2.0, toluene (0.2 M), 100 °C

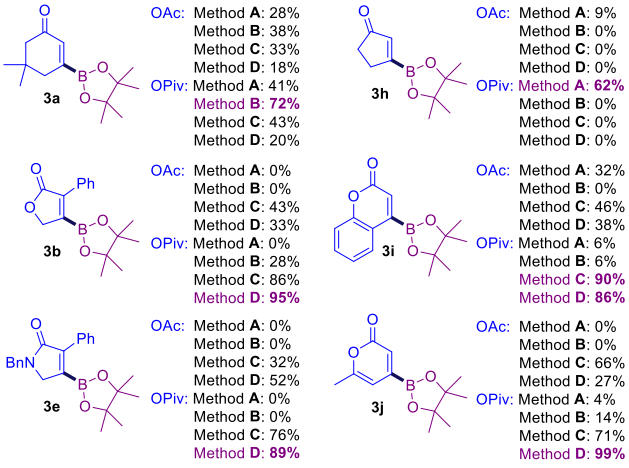

Fig. 5. Comparison of Pd-catalyzed methods for base-free Miyaura borylation of alkenyl acetate and pivalate substrates. Substrate loading: 0.12 mmol for Methods A, C-D, 0.88 mmol for Method B. Yields determined by ^{1}H NMR spectroscopy using 1,3,5-trimethoxybenzene internal standard.

stability of lactone substrates **1b** (OAc) and **2b** (OPiv) under Method D conditions (without addition of B_2pin_2) revealed no change to the concentration of either substrate. However, our previous observation of C_{acyl} – O oxidative addition as a competitive pathway for alkenyl acetate substrates led us to prioritize the alkenyl pivalate substrates for further study [46].

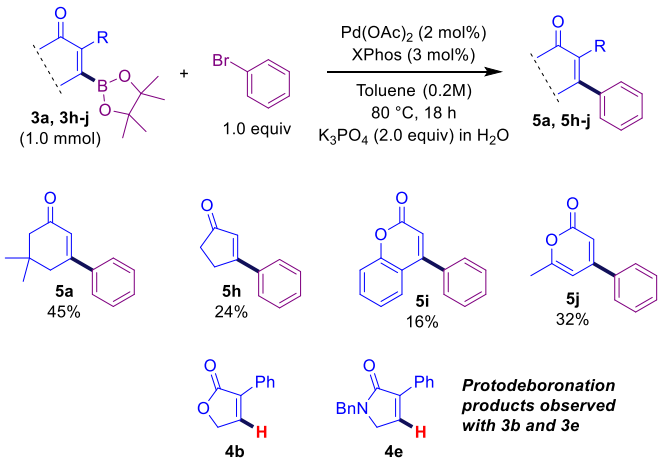

Fig. 6. Suzuki-Miyaura cross-coupling of prepared alkenyl boronates. Yields are for isolated compounds over two steps after column chromatography.

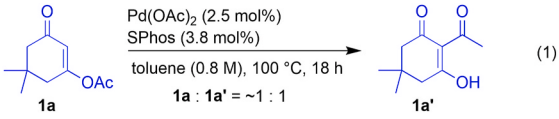

The second major mechanistic question is why different alkenyl pivalate substrates function best under different catalytic methods (**A**, **B**, **C**, or **D**). Whether using a Pd(II) or Pd(0) source, it is likely that these reactions all proceed via a Pd(0)/(II) catalytic cycle, with Pd(II) precursors undergoing reduction by B_2Pin_2 to initiate catalysis [55]. Since C–O oxidative addition to Pd(0) is likely to be turnover-limiting in these reactions, we studied the stoichiometric oxidative addition of the six pivalate substrates from Fig. 5 (**2a**, **b**, **e**, **h-j**) using *in situ* $^{31}P\{^1H\}$ NMR spectroscopy (Fig. 7). We used $Pd(PCy_3)_2$ as the Pd(0) precursor due to its relevant to Methods **C** and **D**, where it is used directly (**C**) or generated *in situ* (**D**); these methods are also the most general, with **2a** and **2h** as 'outliers' in requiring Methods **B** and **A** respectively. Oxidative addition rates are established by tracking the consumption of $Pd(PCy_3)_2$ as well as the generation of a new ^{31}P-containing species, which we assign as the oxidative addition complexes **7**. As support for these assignments, the ^{31}P NMR chemical shift for compound **7j** was identical to that previously determined by our group on an isolated sample [46]. We also previously isolated and characterized a close analogue of **7a** (derived from the alkenyl pivalate of cyclohexa-1,3-dione) [48], which exhibits a very similar ^{31}P NMR chemical shift to that observed here. $^{31}P\{^1H\}$ NMR spectral data for each oxidative addition time-course experiment is given in the Supplementary Information.

From these data, it is clear that substrate structure has a significant effect on oxidative addition rates, which span at least two orders of magnitude under these conditions (Table 1). Furthermore, the propensity for each substrate to undergo oxidative addition, as well as the stability of the resulting complex, offer insights into why specific methods are most suitable for borylation. On one end of the reactivity scale, dimedone-derived substrate **2a** is nearly inert under these conditions, with no **7a** observed after 3 h; however, after 20 h we observe 25 % consumption of $Pd(PCy_3)_2$ and concomitant formation of **7a**, though only in trace amounts. This is consistent with our prior studies on alkenyl pivalate oxidative addition, which established that 60–80 °C and 24–72 h is required for C–O activation of similar cyclohexanone substrates[47,48]. Since **2a** is so poorly reactive toward $Pd(PCy_3)_2$ *vis-à-vis* the other substrates, it is reasonable that alternative conditions employing a more advanced phosphine ligand (SPhos, identified during targeted screening) would be more effective. The recalcitrance of **2a** to undergo C–O oxidative addition also explains why Pd(II) sources appear superior: the two Pd(0) sources tested contain electron-deficient alkene stabilizers (dba, MAH), which may act as competitive inhibitors to further reduce the rate of C–O oxidative addition.

In contrast, the cyclopentenyl substrate **2h** exhibits rapid oxidative addition reactivity with $Pd(PCy_3)_2$ under these conditions; however, we observe *two* new signals in the $^{31}P\{^1H\}$ NMR spectra (one 'major' and one 'minor') rather than one. Furthermore, these species both degrade after 20 h at 50 °C (some decomposition is already evident from 2 to 3 h). It therefore appears that the oxidative addition intermediate derived

Table 1
Relative oxidative addition rates (k_{rel}) for alkenyl pivalates **2** to $Pd(PCy_3)_2$.

Substrate	2a	2e	2j	2i	2b	2h
k_{rel}[a]	<0.1	1	2.2	2.4	5.7	9.8[b]

[a] k_{rel} defined as initial rate (h^{-1}) of $Pd(PCy_3)_2$ consumption over 3 h reaction time for oxidative addition of a given substrate (linear slope of data from Fig. 6, $Pd(PCy_3)_2$ consumption) normalized to initial rate of $Pd(PCy_3)_2$ consumption for oxidative addition of **2e** (defined as $k_{rel} = 1$).

[b] Initial rate for **2h** oxidative addition estimated from only 1 h reaction time due to non-linearity.

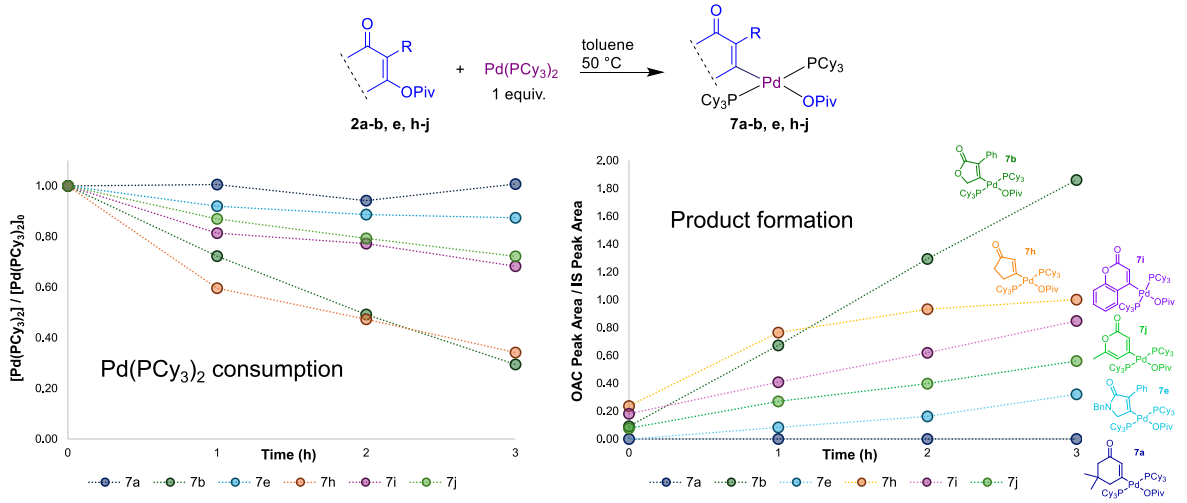

Fig. 7. Initial rates (over 3 h) for oxidative addition of alkenyl pivalates **2a**, **b**, **e**, **h-j** to $Pd(PCy_3)_2$ at 50 °C. Reaction progress monitoring performed by *in situ* $^{31}P\{^1H\}$ NMR spectroscopy using a sealed capillary of PPh_3 dissolved in C_6D_6 as an internal standard.

from **2h** is thermally unstable, which is consistent with only the most mild reaction conditions (Method **A**, which operates at room temperature) being suitable.

Among the four heterocyclic pivalates, all of which function well with a Pd(0)/PCy_3 catalyst system, we observe a significant rate difference between addition of lactone **2b** and lactam **2e**. The lactone reacts 6-fold faster than the lactam, which likely reflects the stronger electron-withdrawing ability of the ester versus the amide. This is consistent with our prior analysis of oxidative addition reactivity trends as a function of molecular electrostatic potentials, where a more electron-deficient carbon center leads to faster oxidative addition [57, 58]. The coumarin (**2j**) and pyrone (**2i**) substrates undergo oxidative addition approximately 2-fold faster than the lactam. The reasonable oxidative addition rates for these four substrates with $Pd(PCy_3)_2$, and the stability of the resulting complexes, are consistent with the suitability of Methods **C** and **D** for these borylation reactions.

Due to the well-behaved nature of **2b** toward oxidative addition, we were able to isolate and characterize the resulting Pd(II) complex, including by X-ray crystallography. The solid-state molecular structure of **7b** is shown in Fig. 8, confirming its composition as a four-coordinate, square planar bis(phosphine) complex with *trans*-PCy_3 ligands. The pivalate ligand binds in a κ^1-*O* fashion *trans* to the alkenyl ligand, which is oriented perpendicular to the Pd/ligand plane. Importantly, this complex undergoes rapid and complete transmetallation with B_2Pin_2 at room temperature (observed by ^1H and $^{31}P\{^1H\}$ spectroscopy). This experiment was performed in d^8-THF to ensure solubility of **7b** (which crystallizes from toluene at rt). Within minutes of treating **7b** with excess B_2Pin_2, we observe formation of $Pd(PCy_3)_2$ as well as borylated lactone **3b** along with a minor amount of protodeborylated **4b**. This experiment confirms that C–O oxidative addition is turnover-limiting in these reactions, and that direct transmetallation of palladium pivalate intermediates with B_2Pin_2 is feasible without addition of a base to activate the boron reagent.

Finally, the mechanistic differences observed for these 12 exemplar substrate classes (six scaffolds with either acetate or pivalate leaving groups), including substrate/intermediate stability and rates of C–O activation via oxidative addition, highlights the importance of including substrate identity as a variable when evaluating new synthetic methods [59]. By performing multifactor screening across multiple substrates, both generally-applicable conditions (i.e. Methods C and D) and specific 'outlier' conditions (Methods A and B) can be quickly identified.

2.3. Protodeboronation as a means of net-deoxygenation

Protodeboronation of **3b** and **3e** to afford **4b** and **4e**, even under controlled stoichiometric conditions for **3b** (Fig. 8), led us to investigate the stability of the corresponding boronates to simple aqueous work-up procedures. We discovered that γ-lactone and γ-lactam alkenyl boronates are extremely sensitive to even mild aqueous base, undergoing significant deboronation after a saturated $NaHCO_3$ wash. This is consistent with the deboronation observed during attempted Suzuki-Miyaura coupling, which uses an aqueous base.

Boronic ester functional groups are often used as a more robust alternative to the boronic acid [60–63]. The Lloyd-Jones group has completed a thorough investigation of the protodeboronation of (hetero)arylboronic esters, where they conclude that factors leading to deboronation are multi-faceted, with several operative mechanisms that depend on if the solution pH is close to the pK_a of the boronic ester [60].

While the observed deboronation renders these compounds unsuitable for standard Suzuki-Miyaura cross-coupling, it does result in a net-deoxygenation process. Overall, the corresponding enol pivalates – readily generated by standard condensation chemistry – are acylated, borylated, and then deborylated to effectively replace –OH with –H. Furthermore, this reduction is selective, leaving other reducible groups (C═C and C═O) intact. After reviewing the literature for other cases where alkenyl carboxylates were deoxygenated, we identified a single report where a δ-lactone was deoxygenated through a process involving harsh acidic conditions and multiple steps [64]. Others have utilized the limited stability of boronic esters to deboronate selectively [65], but use of deboronation as a desired synthetic method remains underdeveloped.

This led us to optimize the protodeboronation conditions for the set of six γ-lactone and γ-lactam boronates, as many biologically active molecules contain the γ-lactone and γ-lactam motif [66–69]. Furthermore, the resulting deoxygenated γ-lactones would be valuable coupling partners in asymmetric allylic alkylation (AAA) chemistry [70], while the unsubstituted γ-lactams have been used in Michael additions [71].

Using Method **D** to borylate the **2b-g** to generate **3b-g**, five aqueous solutions of varying pH and ionic strength were tested for protodeboronation under biphasic conditions (toluene as the organic solvent) (Fig. 9). The solutions were basic (saturated Na_2CO_3, saturated $NaHCO_3$), neutral (saturated NaCl, H_2O), and acidic (5 % HCl). Very little deboronation was found to occur with the saturated NaCl and 5 % HCl solutions, while neutral H_2O led to increased formation of **4b-g**. Under basic conditions, much higher extents of deboronation are

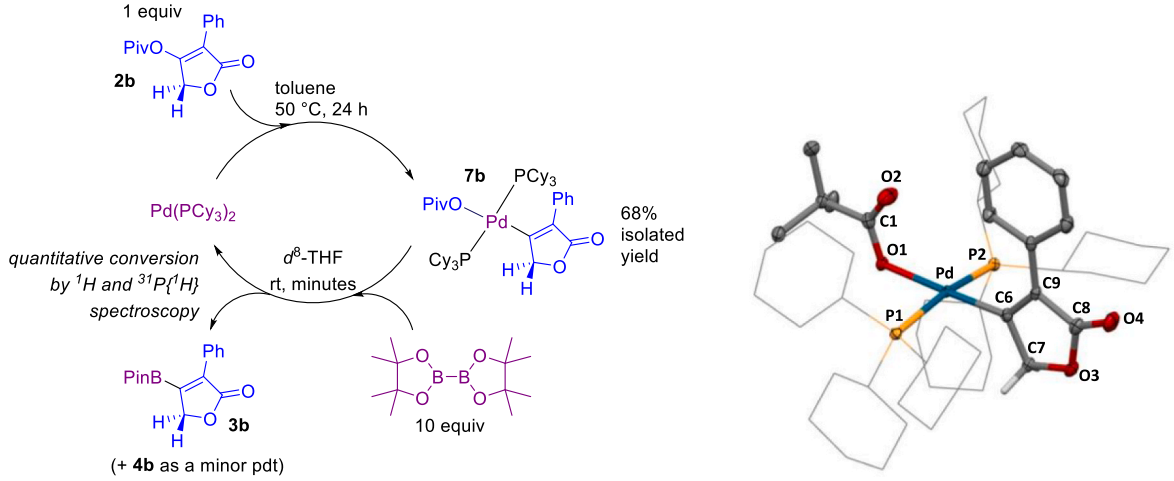

Fig. 8. *Left:* Synthesis of **7b** by oxidative addition, and transmetallation with B_2Pin_2. *Right:* Solid-state molecular structure of **7b** from X-ray crystallography. Ellipsoids at 50 % probability; Cy groups shown as wireframe; hydrogens (except on C7) and toluene molecule removed for clarity.

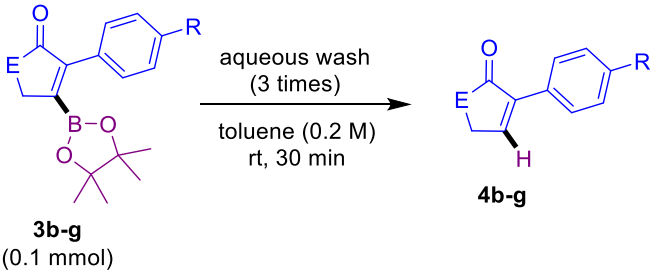

	% Yield	sat Na_2CO_3	sat $NaHCO_3$	sat NaCl	H_2O	5% HCl
4b	>98	>98	7	20	8
4c	>98	81	7	12	7
4d	>98	>98	9	34	10
4e	47	69	12	40	22
4f	46	41	19	45	21
4g	77	85	11	61	12

Fig. 9. Protodeboronation of alkenyl boronates using aqueous solutions. Yields are represented as ratios of protodeboronated product: alkenyl boronate starting material, determined by ^{1}H NMR spectroscopy.

observed, as measured by the ratio between **3** and **4** by NMR spectroscopy. However, when determining solution yields for all products with an internal standard, we observed a discrepancy with the mass balance. When using Na_2CO_3, the amount of product was significantly reduced for both the γ-lactones and lactams. Use of saturated $NaHCO_3$ led to missing mass balance specifically for the γ-lactones, which we suspected was due to product partitioning between the aqueous and organic phases. Acidification of the aqueous solutions and extraction with ethyl acetate confirmed this, as we recovered additional deboronated product. Accordingly, treatment with saturated $NaHCO_3$ was found to yield the best deboronation results for both γ-lactones and γ-lactams, but required a back extraction for the γ-lactones to achieve high yields.

A slight modification of stirring the biphasic solution overnight at 40 °C enabled scaling up of this procedure. This two-step method was then applied to a scope of γ-lactones and γ-lactams which resulted in moderate isolated yields for the γ-lactones (37–52 %) and good isolated yields for the γ-lactams (75–82 %) (Fig. 10).

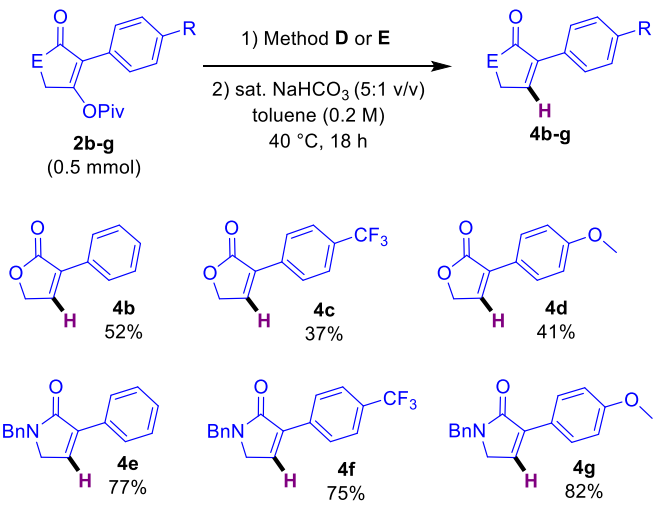

Fig. 10. Protodeboronation of alkenyl pivalate substrates. Yields are for isolated compounds over two steps after column chromatography.

2.4. Achieving stability with an alternative boronic ester, B_2EPin_2

The instability of the boronates **3b-g**, while advantageous in the deoxygenation sequence, is clearly a liability for achieving other transformations of the organoboron group. To alleviate this, we sought alternative boronate groups that would be more robust toward protodeboronation. In particular, a recent account of arylboronic esters based on 3,4-diethyl-hexa-3,4-diol ("ethylpinacol" EPin) [51] caught our attention due to improved stability during column chromatography. The ethyl groups (which replace the methyls of the standard BPin) are hypothesized to sterically block the empty 2*p* orbital on the boron [51], reducing the likelihood of deboronation due to attack on the boron. Notably, while B_2EPin_2 is reported to function in a standard Pd-catalyzed Miyaura borylation, its reactivity in late stage modifications has yet to be evaluated.

We began by synthesizing B_2EPin_2, where we improved the reported literature yield from 25 % to 55 % with a revised work-up and isolation procedure for 3,4-diethyl-hexa-3,4-diol (See Supporting Information). We then substituted B_2EPin_2 for B_2Pin_2 in our optimized borylation methods for γ-lactones and γ-lactams (**2b-g**) (Fig. 11). In all cases, the desired product (**6b-g**) was generated in moderate to good solution yields. γ-Lactones **2b-d** gave comparable yields (80–81 %) to their BPin counterparts; however γ-lactams saw an overall decrease in yield (48–83 %, 65 % average). Importantly, all six alkenyl-BEPin products are stable to aqueous work-up, and to column chromatography, which is a marked improvement on their BPin counterparts.

Finally, in an effort to test the reactivity of the BEPin group for cross-coupling, the methoxy substituted γ-lactone **6d** was taken forward with the same generic cross-coupling procedure of Fig. 6 (eq. (2)). This proved effective, however ethyl pinacol and another unidentified impurity remained in the crude reaction mixture (See Supporting Information). Reforming B_2EPin_2 through a reaction with $B_2(OH)_4$ removed one of the impurities while allowing us to recycle the difficult to synthesize ethyl pinacol for future reactions. The second impurity HBEPin partially coeluted on a silica column with the product resulting in a reduced yield. Further efforts to remove this HBEPin impurity with

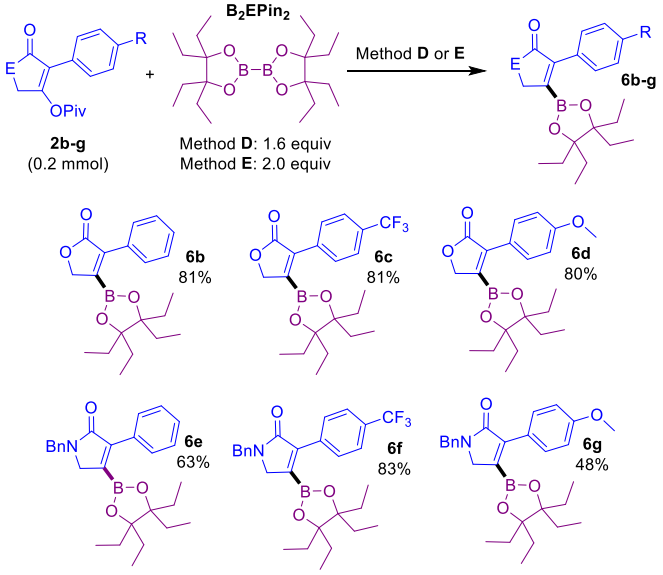

Fig. 11. Base-free Miyaura borylation of alkenyl pivalates. Yields determined by ^{1}H NMR spectroscopy using 1,3,5-trimethoxybenzene as internal standard.

selective extractions, crystallizations, or distillations were also unsuccessful.

(2)

3. Conclusion

This article describes the base-free Pd-catalyzed borylation of alkenyl carboxylates utilizing two tetraalkoxydiboron sources. Depending on the boron source, the reactivity and stability of the resulting alkenyl boronate differs and therefore allows for the synthesis of distinct classes of compounds. We report seven borylation procedures, one using the Leitch Lab's recently reported catalyst: ^{DMP}DAB-Pd-MAH and PCy_3 as an *in situ* system. Further studies on the mechanism are currently underway.

4. Experimental section

4.1. General considerations

All solvents and chemicals were purchased from commercial suppliers and used without any further purification. All air-free manipulations were performed under a nitrogen atmosphere using an MBraun glovebox. Palladium (II) acetate, bis(tricyclohexylphosphine) palladium (0), Dichloro 1,1′-bis(diphenylphosphino)ferrocene palladium (II) dichloromethane, P(*o*-MeOPh)$_3$, XPhos, SPhos, and dppf were purchased from Strem Chemicals and stored under inert atmosphere. B_2Pin_2 was purchased from AK Scientific and stored under inert atmosphere. High-throughput screening experiments were performing using sealable aluminum reaction blocks obtained from Analytical Sales Inc. Heating/stirring was achieved using rare-earth magnetic tumble stirrers obtained from V&P Scientific. All NMR spectra were acquired on either a Bruker AVANCE 300 MHz spectrometer or a Bruker AVANCE Neo 500 MHz spectrometer. All ^{1}H and ^{13}C chemical shifts are calibrated to residual protio-solvents. All data is processed using Bruker TopSpin 4.07. HRMS data was acquired on a Thermo Scientific Ultimate 3000 ESI-Orbitrap Exactive Plus.

4.2. Experimental procedures

4.2.1. General procedure for synthesis of lactone starting materials

Step 1: A round bottom flask was charged with substituted phenyl acetic acid (1.0 equiv, [12.0 mmol]), triethyl amine (1.0 equiv, [1.22 g, 1.68 mL]), and THF (0.65 M [18.5 mL]). To the stirred solution ethyl bromoacetate (1.0 equiv, [2.01 g, 1.33 mL]) was added dropwise via syringe. The reaction was then stirred at 70 °C overnight. The reaction mixture was transferred to a separatory funnel and diluted with ethyl acetate (~2x (v/v) dilution [40 mL]), and H_2O (~2x (v/v) dilution [40 mL]). The organic phase is washed 3x with H_2O [40 mL]. The collected organic phase is dried with $MgSO_4$, filtered, and evaporated to dryness.

Step 2: We found in order to optimize the yield of this reaction, that the maximum scale this step could be performed at was 3.5 mmol scale. Thusly this reaction was performed at larger scale in multiple 4-dram vials. Potassium tert-butoxide (1.2 equiv) was evenly divided among the appropriate number of 4-dram vials. THF (0.375 M) was dispensed into each vial. The esterification product synthesized in Step 1 was dissolved in THF (1/4 of previous amount in solution – net result is 0.3 M solution) and added dropwise evenly to the 4-dram vials. The 4-dram vials were sealed (with Teflon lined lids) and allowed to stir vigorously at 110 °C for 48 h. The reaction mixtures were evaporated to dryness and resuspended in 1 M NaOH. The combined reaction mixtures were washed twice with hexanes. The aqueous phase was acidified slowly using 1 M HCl, until the product had fully precipitated out of solution. The product was collected by filtration, washing with hexanes. DMSO-d_6 used for ^{1}H NMR spectroscopy analysis.

Step 3: A round bottom flask was charged with the cyclized product from Step 2 (1.0 equiv), DIPEA (1.2 equiv), and DCM (0.3 M). Trimethylacetyl chloride (1.1 equiv) was added dropwise to the stirred solution and allowed to stir overnight at room temperature. The resulting organic phase was washed 3x with 1 M HCl, 3x with saturated sodium bicarbonate, and dried with $MgSO_4$, before filtering and evaporating to dryness. The resulting oil was then triturated with hexanes to yield a colourless solid that can be analyzed by ^{1}H NMR spectroscopy in $CDCl_3$.

4.2.1.1. 4-Pivalyloxy-3-(4-trifluoromethyl)phenylpyran-3-en-2-one (2c). Step 1 was performed at 12.0 mmol scale [4-(trifluoromethyl)phenylacetic acid: 2.45 g], to produce 1.89 g, 48 % yield after Step 3. ^{1}H NMR (500 MHz, $CDCl_3$, 292 K, ppm): δ 7.95 (d, J = 8.2 Hz, 2H), 7.68 (d, J = 8.2 Hz, 2H), 5.31 (s, 2H), 1.35 (s, 9H). ^{13}C NMR (126 MHz, $CDCl_3$, 292 K, ppm): δ 173.8, 170.4, 165.6, 131.6, 130.5 (q, J = 32.7 Hz), 128.6, 125.4 (q, 3.7 Hz), 124.0 (q, J = 272.7 Hz), 109.1, 67.8, 39.7, 26.9. ^{19}F NMR (282 MHz, CDCl3, 292 K, ppm): δ −62.9. HRMS: Calc'd for $C_{16}H_{15}F_3O_4$ $[M+Na]^+$: 351.08146; found: 351.08148.

4.2.1.2. 3-(4-methoxyphenyl)-4-pivalyloxypyran-3-en-2-one (2d). Step 1 was performed at 12.0 mmol scale [4-(methoxy)phenylacetic acid: 2.0 g], to produce 1.35 g, 39 % yield after Step 3. ^{1}H NMR (500 MHz, $CDCl_3$, 292 K, ppm): δ 7.66 (d, J = 8.9 Hz, 2H), 6.78 (d, J = 9.0 Hz, 2H), 5.01 (s, 2H), 3.63 (s, 3H), 1.20 (s, 9H). ^{13}C NMR (126 MHz, $CDCl_3$, 292 K, ppm): δ 173.8, 170.8, 162.6, 159.5, 129.3, 120.4, 113.6, 109.4, 67.3, 55.0, 39.3, 26.7. HRMS: Calc'd for $C_{16}H_{18}O_5$ $[M+Na]^+$: 313.10464; found: 313.10466.

4.2.2. General procedure for synthesis of lactam starting materials

Step 1: A round bottom flask was charged with *N*-benzyl glycine ethyl ester (1.0 equiv [1.74 g, 1.64 mL]), DIPEA (1.5 equiv [1.74 g, 2.35 mL]), and toluene (0.5 M [18.0 mL]). The substituted phenylacetyl chloride (1.0 equiv [9.0 mmol]), was dissolved in toluene (equal amount to what is previously in solution – net result is 0.25 M solution [18.0 mL]), and added dropwise to the stirred reaction. The stirred solution was then heated to 60 °C for 2 h, then allowed to stir overnight at room temperature. The reaction mixture was washed with a solution of 50 % saturated NH_4Cl and 50 % H_2O [30 mL], then H_2O [30 mL], and then saturated aqueous NaCl solution [30 mL]. The organic layer was dried with $MgSO_4$, filtered and evaporated to dryness. The crude product was taken forward in the next step.

Step 2: We found in order to optimize the yield of this reaction, that the maximum scale this step could be performed at was 3.5 mmol scale. Thusly this reaction was performed at larger scale in multiple 4-dram vials. Potassium tert-butoxide (1.2 equiv) was evenly divided among the appropriate number of 4-dram vials. THF (0.375 M) was dispensed into each vial. The alkylated amine synthesized in Step 1 was dissolved in THF (1/4 of previous amount in solution – net result is 0.3 M solution) and added dropwise evenly to the 4-dram vials. The 4-dram vials were sealed (with Teflon lined lids) and allowed to stir vigorously at 110 °C for 48 h. The reaction mixtures were evaporated to dryness and resuspended in 1 M NaOH. The combined reaction mixtures were washed twice with hexanes. The aqueous phase was acidified slowly using 1 M HCl, until the product had fully precipitated out of solution. The product was collected by filtration, washing with hexanes. DMSO-d_6 used for ^{1}H NMR spectroscopy analysis.

Step 3: A round bottom flask was charged with the cyclized product from Step 2 (1.0 equiv), DIPEA (1.2 equiv), and DCM (0.3 M). Trimethylacetyl chloride (1.1 equiv) was added dropwise to the stirred solution and allowed to stir overnight at room temperature. The collected organic phase was washed 3x with 1 M HCl, 3x with saturated sodium

bicarbonate, and dried with $MgSO_4$, before filtering and evaporating to dryness. The resulting oil was then triturated with hexanes to yield a colourless solid that can be analyzed by ^{1}H NMR spectroscopy in $CDCl_3$.

4.2.2.1. 1-Benzyl-4-pivalyloxy-3-(4-trifluoromethylphenyl)pyrrolidin-3-en-2-one (2f). Step 1 was performed at 9.0 mmol scale [4-(trifluoromethyl)benzeneacetyl chloride: 2.0 g], to produce 1.65 g, 44 % yield after Step 3. ^{1}H NMR (500 MHz, $CDCl_3$, 292 K, ppm): δ 7.96 (d, J = 8.2 Hz, 2H), 7.67 (d, J = 8.3 Hz, 2H), 7.33 (m, 5H), 4.71 (s, 2H), 4.30 (s, 2H), 1.29 (s, 9H). ^{13}C NMR (126 MHz, $CDCl_3$, 292 K, ppm): δ 174.5, 168.4, 158.8, 136.9, 133.2, 129.9 (q, J = 32.6 Hz), 129.0, 128.9, 128.3, 127.9, 125.2 (q, J = 3.8 Hz), 124.2 (q, J = 272.3 Hz), 49.5, 46.0, 39.6, 27.0. ^{19}F NMR (282 MHz, $CDCl_3$, 292 K, ppm): δ −62.7. HRMS: Calc'd for $C_{23}H_{22}F_3NO_3$ $[M+Na]^+$: 440.14440; found: 440.14441.

4.2.2.2. 1-Benzyl-4-pivalyloxy-3-(4-methoxyphenyl)pyrrolidin-3-en-2-one (2g). Step 1 was performed at 9.0 mmol scale[4-(methoxy)benzeneacetyl chloride: 1.66 g], to produce 2.13 g, 62 % yield after Step 3. ^{1}H NMR (500 MHz, $CDCl_3$, 292 K, ppm): δ 7.85 (d, J = 8.8 Hz, 2H), 7.27 (m, 5H), 6.95 (d, J = 8.8 Hz, 2H), 4.67 (s, 2H), 4.21 (s, 2H), 3.77 (s, 3H), 1.27 (s, 9H). ^{13}C NMR (126 MHz, $CDCl_3$, 292 K, ppm): δ 174.4, 168.9, 159.2, 155.8, 136.9, 129.7, 128.5, 127.9, 127.4, 121.8, 117.0, 113.4, 54.9, 48.9, 45.6, 39.1, 26.7. HRMS: Calc'd for $C_{23}H_{25}NO_4$ $[M+H]^+$: 380.18564; found: 380.1857.

4.2.3. Synthesis of 3,4-Diethylhexane-3,4-diol

Caution: Read appropriate SDS before conducting this synthesis. Reaction should be performed in a fume hood. HCl gas if formed, the open neck of the flask should point towards the back of the fume hood.

A two-necked round bottom flask was charged with Mg turnings (1.92 g, 78.95 mmol, 2 equiv), this was flushed with N_2 thoroughly before 60 mL anhydrous THF added to flask. The flask was then cooled to 0 °C. While under constant N_2 flow (through septum on one neck of flask – other neck of flask open and pointing into back of fume hood) $TiCl_4$ (5.2 mL, 47.37 mmol, 1.2 equiv) was added dropwise (through septum with N_2). Once complete, another 30 mL anhydrous THF was used to wash contents down in flask. After 30 min, 0 °C was maintained, and 3-pentanone (4.2 mL, 39.48 mmol, 1 equiv) was added dropwise slowly. The reaction mixture was allowed to stir overnight and allowed to reach room temperature. The reaction was then quenched slowly with saturated Na_2CO_3 solution (~150 mL). Once gas evolving ceased, the reaction mixture was filtered through a pad of silica under vacuum. Dichloromethane (~400 mL) was used to wash product through while constantly manually stirring with a spatula. The eluent was then extracted with diethyl ether, creating a triphasic mixture. Both organic layers were removed, dried with $MgSO_4$, filtered and evaporated to dryness to yield the final product (1.88g, 55 % yield).

4.2.4. Synthesis of Lactone alkenyl pinacol boronates

Under N_2 atmosphere, a 1 dram vial was charged with the respective lactone alkenyl carboxylate precursor (0.50 mmol), B_2Pin_2 (203.2 mg, 0.80 mmol), ^{DMP}DAB-Pd-MAH (8.2 mg, 0.018 mmol), PCy_3 (9.8 mg, 0.035 mmol), and toluene (2.5 mL, 0.2 M in alkenyl carboxylate). The reaction mixture was stirred at 100 °C for 18 h. The solutions were then evaporated to dryness, and NMR spectroscopic analysis conducted in $CDCl_3$ (0.6 mL).

4.2.4.1. 4-(4,4,5,5-Tetramethyl-1,3,2-dioxaborolan-2-yl)-3-(4-(trifluoromethyl)phenyl)furan-2(5H)-one (3c). ^{1}H NMR (500 MHz, $CDCl_3$, 292 K, ppm): δ 7.81 (d, J = 8.2 Hz, 2H), 7.63 (d, J = 8.3 Hz, 2H), 4.99 (s, 2H), 1.27 (s, 12H). ^{13}C NMR (126 MHz, $CDCl_3$, 292 K, ppm): δ 173.07, 139.20, 134.05, 131.09 (q, J = 32.6 Hz), 129.78, 126.75, 124.90 (q, J = 3.6 Hz) 85.24, 73.16, 24.78. ^{19}F NMR (282 MHz, $CDCl_3$, 292 K, ppm): δ −62.78. HRMS: Calc'd for $C_{17}H_{18}BF_3O_4$ $[M+H]^+$: 355.13230; found: 355.13223.

4.2.4.2. 3-(4-methoxyphenyl)-4-(4,4,5,5-tetramethyl-1,3,2-dioxaborolan-2-yl)furan-2(5H)-one (3d). ^{1}H NMR (500 MHz, $CDCl_3$, 292 K, ppm): δ 7.71–7.67 (m, 2H), 6.90–6.87 (m, 2H), 4.92 (s, 2H), 3.81 (s, 3H), 1.27 (s, 12H). ^{13}C NMR (126 MHz, $CDCl_3$, 292 K, ppm): δ 173.82, 139.68, 130.82, 128.40, 123.17, 113.42, 84.85, 72.86, 55.33, 24.78. HRMS: Calc'd for $C_{17}H_{21}BO_5$ $[M+H]^+$: 317.15548; found: 317.15528.

4.2.5. Synthesis of lactam alkenyl pinacol boronates

Under N_2 atmosphere, a 1 dram vial was charged with the respective lactam alkenyl carboxylate precursor (0.50 mmol), B_2Pin_2 (253.9 mg, 1.00 mmol), ^{DMP}DAB-Pd-MAH (11.7 mg, 0.025 mmol), PCy_3 (14.0 mg, 0.05 mmol), and toluene (2.5 mL, 0.2 M in alkenyl carboxylate). The reaction mixture was stirred at 100 °C for 18 h. The solutions were then evaporated to dryness, and NMR spectroscopic analysis conducted in $CDCl_3$ (0.6 mL).

4.2.5.1. 1-Benzyl-4-(4,4,5,5-tetramethyl-1,3,2-dioxaborolan-2-yl)-3-(4-(trifluoromethyl)phenyl)-1,5-dihydro-2H-pyrrol-2-one (3f). ^{1}H NMR (500 MHz, $CDCl_3$, 292 K, ppm): δ 7.84 (d, J = 8.1 Hz, 2H), 7.64 (d, J = 8.2 Hz, 2H), 7.38–7.24 (m, 5H), 4.73 (s, 2H), 4.04 (s, 2H), 1.25 (s, 12H). ^{13}C NMR (126 MHz, $CDCl_3$, 292 K, ppm): δ 169.96, 146.26, 137.5, 137.12, 135.94, 130.37 (d, J = 32.3 Hz), 130.02, 128.87, 128.40, 127.78, 124.56 (q, J = 3.8 Hz), 84.58, 53.47, 46.93, 24.73. ^{19}F NMR (282 MHz, $CDCl_3$, 292 K, ppm): δ −62.59. HRMS: Calc'd for $C_{24}H_{28}BF_3NO_3$ $[M+H]^+$: 444.19524; found: 444.19512.

4.2.5.2. 1-Benzyl-3-(4-methoxyphenyl)-4-(4,4,5,5-tetramethyl-1,3,2-dioxaborolan-2-yl)-1,5-dihydro-2H-pyrrol-2-one (3g). ^{1}H NMR (500 MHz, $CDCl_3$, 292 K, ppm): δ 7.73–7.70 (m, 2H), 7.35–7.23 (m, 5H), 6.93–6.89 (m, 2H), 4.71 (s, 2H), 3.97 (s, 2H), 3.84 (s, 3H), 1.25 (s, 12H). ^{13}C NMR (126 MHz, $CDCl_3$, 292 K, ppm): δ 170.65, 137.37, 131.02, 128.78, 128.74, 128.33, 128.14, 127.58, 125.07, 113.12, 84.19, 55.27, 53.14, 46.83, 24.71. HRMS: Calc'd for $C_{24}H_{28}BNO_4$ $[M+H]^+$: 406.21842; found: 406.21816.

4.2.6. Synthesis of deboronated products

Borylation methods described in Sections 4.2.4 and 4.2.5 were performed on the appropriate lactone or lactam alkenyl carboxylate before the following deboronation procedure:

The appropriate alkenyl boronate **3** was resuspended in a 4-dram vial with toluene (2.5 mL, 0.2 M in substrate). Saturated aqueous $NaHCO_3$ (2.5 mL, (1:1 v/v to toluene)) was dispensed into the vial. The reaction mixture was allowed to stir vigorously at 40 °C overnight. The reaction mixture was then transferred to a separatory funnel using toluene and H_2O. The aqueous phase was acidified using 5 % HCl solution to pH = 2, extracted with ethyl acetate (~10 mL) twice. The combined organic fractions were dried using $MgSO_4$ and evaporated to dryness before column chromatography using Biotage Selekt instruments (detailed in the ESI).

4.2.6.1. 1-Benzyl-3-(4-(trifluoromethyl)phenyl)-1,5-dihydro-2H-pyrrol-2-one (4f). ^{1}H NMR (500 MHz, $CDCl_3$, 292 K, ppm): δ 8.06 (d, J = 8.1 Hz, 2H), 7.67 (d, J = 8.2 Hz, 2H), 7.38–7.35 (m, 2H), 7.32–7.29 (m, 4H), 4.74 (s, 2H), 3.96 (d, J = 2.1 Hz, 2H).^{13}C NMR (126 MHz, $CDCl_3$, 292 K, ppm): δ 169.48, 137.53, 137.14, 136.00, 135.30, 130.38 (q, J = 32.4 Hz), 128.94, 128.19, 127.82, 127.39, 125.44 (q, J = 3.8 Hz), 124.24 (d, J = 272.1 Hz), 50.02, 46.54. ^{19}F NMR (282 MHz, $CDCl_3$, 292 K, ppm): δ −62.65. HRMS: Calc'd for $C_{18}H_{14}F_3NO$ $[M+H]^+$: 318.11003; found: 318.10980.

4.2.6.2. 1-Benzyl-3-(4-methoxyphenyl)-1,5-dihydro-2H-pyrrol-2-one (4g). ^{1}H NMR (500 MHz, $CDCl_3$, 292 K, ppm): δ 7.98–7.86 (m, 2H), 7.38–7.33 (m, 2H), 7.32–7.28 (m, 3H), 7.07 (t, J = 2.2 Hz, 1H), 6.97–6.91 (m, 2H), 4.73 (s, 2H), 3.88 (d, J = 2.2 Hz, 2H), 3.85 (s, 3H). ^{13}C NMR (126 MHz, $CDCl_3$, 292 K, ppm): δ 170.26, 159.90, 137.45,

136.27, 133.44, 128.81, 128.34, 128.13, 127.61, 124.60, 113.90, 55.35, 49.76, 46.44. HRMS: Calc'd for $C_{18}H_{17}NO_2$ $[M+Na]^+$: 302.11515; found: 302.11507.

4.2.7. Synthesis of Lactone and lactam alkenyl ethylpinacol boronates

Borylation methods described in Sections 4.2.4 and 4.2.5 were performed, substituting B_2EPin_2 for B_2Pin_2 at 0.25 mmol scale. (**2b**–**2d**, 4.2.4: B_2EPin_2: 147.1 mg, 0.40 mmol; **2e**–**2g**, 4.2.5: B_2EPin_2: 183.9 mg, 0.50 mmol).

4.2.7.1. 1-(4,4,5,5-Tetraethyl-1,3,2- dioxaborolan-2-yl)-3-phenylpyran-3-en-2-one (6b). ^{1}H NMR (500 MHz, $CDCl_3$, 292 K, ppm): δ 7.74–7.71 (m, 2H), 7.39–7.36 (m, 3H), 4.98 (s, 2H), 1.74–1.63 (m, 8H), 0.88 (t, $J = 7.5$ Hz, 12H). ^{13}C NMR (126 MHz, $CDCl_3$, 292 K, ppm): δ 173.69, 140.48, 130.78, 129.45, 129.27, 127.96, 90.15, 73.15, 26.34, 8.83. HRMS: Calc'd for $C_{20}H_{27}BO_4$ $[M+H]^+$: 343.29752; found: 343.29743.

4.2.7.2. 1-(4,4,5,5-Tetraethyl-1,3,2- dioxaborolan-2-yl) -3-(4-trifluoromethyl)phenylpyran-3-en-2-one (6c). ^{1}H NMR (500 MHz, $CDCl_3$, 292 K, ppm): δ 7.86 (d, $J = 8.2$ Hz, 2H), 7.64 (d, $J = 8.3$ Hz, 2H), 5.01 (s, 2H), 1.75–1.63 (m, 8H), 0.88 (t, $J = 7.5$ Hz, 12H). ^{13}C NMR (126 MHz, $CDCl_3$, 292 K, ppm): δ 173.17, 139.40, 134.21, 131.09 (q, $J = 32.8$ Hz) 129.91, 125.26, 124.87 (q, $J = 3.8$ Hz), 90.46, 73.34, 26.36, 8.82. ^{19}F NMR (282 MHz, $CDCl_3$, 292 K, ppm): δ −62.82. HRMS: Calc'd for $C_{21}H_{26}BF_3O_4$ $[M+H]^+$: 411.19490; found: 411.19477.

4.2.7.3. 1-(4,4,5,5-Tetraethyl-1,3,2- dioxaborolan-2-yl) -3-(4-methoxy) phenylpyran-3-en-2-one (6d). ^{1}H NMR (500 MHz, $CDCl_3$, 292 K, ppm): δ 7.76 (d, $J = 8.9$ Hz, 2H), 6.89 (d, $J = 8.9$ Hz, 2H), 4.94 (s, 2H), 3.83 (s, 3H), 1.74–1.64 (m, 8H), 0.89 (t, $J = 7.5$ Hz, 12H). ^{13}C NMR (126 MHz, $CDCl_3$, 292 K, ppm): δ 174.01, 160.49, 139.78, 131.00, 123.37, 113.41, 90.06, 73.11, 55.43, 26.37, 8.88. HRMS: Calc'd for $C_{21}H_{29}BO_5$ $[M+H]^+$: 373.21808; found: 373.21795.

4.2.7.4. 1-(4,4,5,5-Tetraethyl-1,3,2- dioxaborolan-2-yl) -1-benzyl-3-phenylpyrrolidin-3-en-2-one (6e). ^{1}H NMR (500 MHz, $CDCl_3$, 292 K, ppm): δ 7.73–7.70 (m, 2H), 7.42–7.27 (m, 8H), 4.72 (s, 2H), 4.00 (s, 2H), 1.75–1.58 (m, 8H), 0.84 (t, $J = 7.5$ Hz, 12H). ^{13}C NMR (126 MHz, $CDCl_3$, 292 K, ppm): δ 170.59, 147.62, 137.58, 132.64, 129.71, 128.91, 128.54, 128.36, 127.66, 127.16, 89.47, 53.47, 46.89, 26.29, 8.85. HRMS: Calc'd for $C_{27}H_{34}BNO_3$ $[M+H]^+$: 432.27045; found: 432.27037.

4.2.7.5. 1-(4,4,5,5-Tetraethyl-1,3,2- dioxaborolan-2-yl) -1-benzyl-3-(4-trifluoromethyl)phenylpyrrolidin-3-en-2-one (6f). ^{1}H NMR (500 MHz, $CDCl_3$, 292 K, ppm): δ 7.83 (d, $J = 8.2$ Hz, 2H), 7.61 (d, $J = 8.3$ Hz, 2H), 7.37–7.28 (m, 5H), 4.72 (s, 2H), 4.03 (s, 2H), 1.75–1.58 (m, 8H), 0.83 (t, $J = 7.4$ Hz, 12H). ^{13}C NMR (126 MHz, $CDCl_3$, 292 K, ppm): 170.10, 146.50, 137.32, 130.33 (d, $J = 32.4$ Hz), 130.12, 128.92, 128.38, 128.38, 127.78, 125.48, 124.55 (q, $J = 3.7$ Hz), 89.75, 53.64, 46.94, 26.30, 8.81. ^{19}F NMR (282 MHz, $CDCl^3$, 292 K, ppm): δ −62.67. HRMS: Calc'd for $C_{28}H_{33}BF_3NO_3$ $[M+H]^+$: 500.25784; found: 500.25744.

4.2.7.6. 1-(4,4,5,5-Tetraethyl-1,3,2- dioxaborolan-2-yl) -1-benzyl-3-(4-methoxy)phenylpyrrolidin-3-en-2-one (6g). ^{1}H NMR (500 MHz, $CDCl_3$, 292 K, ppm): δ 7.77–7.74 (m, 2H), 7.36–7.27 (m, 5H), 6.91–6.88 (m, 2H), 4.71 (s, 2H), 3.97 (s, 2H), 3.83 (s, 3H), 1.71–1.59 (m, 8H), 0.86 (t, $J = 7.4$ Hz, 12H). ^{13}C NMR (126 MHz, $CDCl_3$, 292 K, ppm): δ 170.84, 146.88, 137.61, 131.18, 130.03, 128.82, 128.42, 127.61, 125.32, 113.12, 89.37, 55.39, 53.40, 46.87, 26.31, 8.89. HRMS: Calc'd for $C_{28}H_{36}BNO_4$ [M+H]+: 462.28102; found: 462.28077.

4.2.8. Suzuki-Miyaura coupling of ethylpinacol boronates

The borylation method described in Section 4.2.4 was performed substituting B_2EPin_2 for B_2Pin_2 at 0.25 mmol scale (**2d**: B_2EPin_2: 147.1 mg, 0.40 mmol), before the Arylation Procedure:

Under a N_2 atmosphere, a 1 dram vial was charged with the borylated (EPin) lactone from 4.2.4, $Pd(OAc)_2$ (1.1 mg, 0.005 mmol), XPhos (3.6 mg, 0.008 mmol), K_3PO_4 (106.9 mg, 0.50 mmol) and bromobenzene (39.4 mg, 26.8 μL, 0.25 mmol). Toluene (1.25 mL, 0.2 M) was dispensed into the vial and sealed with a septum cap. On the bench, 1.25 mL degassed H_2O was dispensed into the vial and the reaction mixture was allowed to stir vigorously at 80 °C for 18 h. The reaction mixture was then transferred to a separatory funnel using toluene and H_2O, the aqueous layer was extracted with toluene twice (~10 mL). The combined organic fractions were dried using $MgSO_4$, filtered, and evaporated to dryness. To remove the ethylpinacol generated in this reaction, B_2EPin_2 was reformed by the crude product being combined with $B_2(OH)_4$ (18.0 mg, 0.20 mmol), NaOAc (18.5 mg, 0.23 mmol), and a scoop of sodium sulfate as a drying reagent in a 50 mL round bottom flask. Toluene (3.0 mL, 0.08 M) was used to resuspend the reaction mixture, and the round bottom flask was fitted with a condenser and swept with N_2. Under N_2, the reaction mixture was allowed to stir vigorously overnight at 120 °C. The reaction mixture was allowed to cool before filtering and evaporating to dryness before column chromatography using a Biotage Selekt instrument (chromatogram in ESI) to yield **5d** (36.7 mg, 55 % yield).

CRediT authorship contribution statement

Gregory Gaube: Writing – original draft, Methodology, Investigation, Formal analysis, Data curation, Conceptualization. **Douglas L. Miller:** Investigation. **Rowan A. McCallum:** Investigation. **Nahiane Pipaón Fernández:** Methodology, Investigation. **David C. Leitch:** Writing – review & editing, Supervision, Resources, Project administration, Funding acquisition, Conceptualization.

Declaration of competing interest

The authors declare the following financial interests/personal relationships which may be considered as potential competing interests: David Leitch reports financial support was provided by Natural Sciences and Engineering Research Council of Canada. David Leitch reports financial support was provided by Canada Foundation for Innovation. David Leitch reports financial support was provided by British Columbia Knowledge Development Fund. If there are other authors, they declare that they have no known competing financial interests or personal relationships that could have appeared to influence the work reported in this paper.

Acknowledgements

We acknowledge with respect the Lekwungen peoples on whose traditional territory the University of Victoria (UVic) stands, and the Songhees, Esquimalt and WSÁNEĆ peoples whose historical relationships with the land continue to this day. The authors thank UVic, NSERC, CFI, and BCKDF for funding this work. We thank Dr. Tyler Trefz and Christopher Barr for their support at the University of Victoria. We also thank Prof. Nathan D. Schley at Vanderbilt University for X-ray crystallographic analysis of **7b**.

Appendix B. Supplementary data

Supplementary data to this article can be found online at https://doi.org/10.1016/j.tet.2025.134682.

Data availability

Data is provided as Supplementary Information.

References

[1] D.J. Konowalchuk, O.M. Schneider, D.G. Hall, Saturated (C(sp^3)–B) boronic acid derivatives, in: Comprehensive Organic Synthesis III, Elsevier, 2025, https://doi.org/10.1016/B978-0-323-96025-0.00049-1. https://linkinghub.elsevier.com/retrieve/pii/B9780323960250000491.

[2] O.M. Schneider, D.J. Konowalchuk, D.G. Hall, Unsaturated (C(sp^2/sp)–B) boronic acid derivatives, in: Comprehensive Organic Synthesis III, Elsevier, 2025, https://doi.org/10.1016/B978-0-323-96025-0.00050-8. https://linkinghub.elsevier.com/retrieve/pii/B9780323960250000508.

[3] M. Wang, Z. Shi, Methodologies and strategies for selective borylation of C–Het and C–C bonds, Chem. Rev. 120 (2020) 7348–7398, https://doi.org/10.1021/acs.chemrev.9b00384.

[4] S.J. Geier, C.M. Vogels, J.A. Melanson, S.A. Westcott, The transition metal-catalysed hydroboration reaction, Chem. Soc. Rev. 51 (2022) 8877–8922, https://doi.org/10.1039/D2CS00344A.

[5] S. Guria, M.M. Mahamudul Hassan, B. Chattopadhyay, C–H borylation: a tool for molecular diversification, Org. Chem. Front. 11 (2024) 929–953, https://doi.org/10.1039/D3QO01931D.

[6] I.F. Yu, J.W. Wilson, J.F. Hartwig, Transition-metal-catalyzed silylation and borylation of C–H bonds for the synthesis and functionalization of complex molecules, Chem. Rev. 123 (2023) 11619–11663, https://doi.org/10.1021/acs.chemrev.3c00207.

[7] M.M.M. Hassan, S. Guria, S. Dey, J. Das, B. Chattopadhyay, Transition metal–catalyzed remote C—H borylation: an emerging synthetic tool, Sci. Adv. 9 (2023) eadg3311, https://doi.org/10.1126/sciadv.adg3311.

[8] D.G. Brown, J. Boström, Analysis of past and present synthetic methodologies on medicinal chemistry: where have all the new reactions gone? J. Med. Chem. 59 (2016) 4443–4458, https://doi.org/10.1021/acs.jmedchem.5b01409.

[9] S.M. Mennen, C. Alhambra, C.L. Allen, M. Barberis, S. Berritt, T.A. Brandt, A. D. Campbell, J. Castañón, A.H. Cherney, M. Christensen, D.B. Damon, J. Eugenio de Diego, S. García-Cerrada, P. García-Losada, R. Haro, J. Janey, D.C. Leitch, L. Li, F. Liu, P.C. Lobben, D.W.C. MacMillan, J. Magano, E. McInturff, S. Monfette, R. J. Post, D. Schultz, B.J. Sitter, J.M. Stevens, I.I. Strambeanu, J. Twilton, K. Wang, M.A. Zajac, The evolution of high-throughput experimentation in pharmaceutical development and perspectives on the future, Org. Process Res. Dev. 23 (2019) 1213–1242, https://doi.org/10.1021/acs.oprd.9b00140.

[10] Norio Miyaura, Akira Suzuki, Palladium-catalyzed cross-coupling reactions of organoboron compounds, Chem. Rev. 95 (1995) 2457–2483, https://doi.org/10.1021/cr00039a007.

[11] R. Martin, S.L. Buchwald, Palladium-catalyzed Suzuki−Miyaura cross-coupling reactions employing dialkylbiaryl phosphine ligands, Acc. Chem. Res. 41 (2008) 1461–1473, https://doi.org/10.1021/ar800036s.

[12] J. Magano, J.R. Dunetz, Large-scale applications of transition metal-catalyzed couplings for the synthesis of pharmaceuticals, Chem. Rev. 111 (2011) 2177–2250, https://doi.org/10.1021/cr100346g.

[13] M.C. D'Alterio, È. Casals-Cruañas, N.V. Tzouras, G. Talarico, S.P. Nolan, A. Poater, Mechanistic aspects of the palladium-catalyzed Suzuki-Miyaura cross-coupling reaction, Chem. Eur J. 27 (2021) 13481–13493, https://doi.org/10.1002/chem.202101880.

[14] S.E. Hooshmand, B. Heidari, R. Sedghi, R.S. Varma, Recent advances in the Suzuki–Miyaura cross-coupling reaction using efficient catalysts in eco-friendly media, Green Chem. 21 (2019) 381–405, https://doi.org/10.1039/C8GC02860E.

[15] M. Farhang, A.R. Akbarzadeh, M. Rabbani, A.M. Ghadiri, A retrospective-prospective review of Suzuki–Miyaura reaction: from cross-coupling reaction to pharmaceutical industry applications, Polyhedron 227 (2022) 116124, https://doi.org/10.1016/j.poly.2022.116124.

[16] M.J. Buskes, M.-J. Blanco, Impact of cross-coupling reactions in drug discovery and development, Molecules 25 (2020) 3493, https://doi.org/10.3390/molecules25153493.

[17] E.C. Neeve, S.J. Geier, I.A.I. Mkhalid, S.A. Westcott, T.B. Marder, Diboron(4) compounds: from structural curiosity to synthetic workhorse, Chem. Rev. 116 (2016) 9091–9161, https://doi.org/10.1021/acs.chemrev.6b00193.

[18] J. Carreras, A. Caballero, P.J. Pérez, Alkenyl boronates: synthesis and applications, Chem. Asian J. 14 (2019) 329–343, https://doi.org/10.1002/asia.201801559.

[19] P. Nad, A. Mukherjee, Metal-free C–H borylation and hydroboration of indoles, ACS Omega 8 (2023) 37623–37640, https://doi.org/10.1021/acsomega.3c05071.

[20] S. Rej, N. Chatani, Regioselective transition-metal-free C(sp2)−H borylation: a subject of practical and ongoing interest in synthetic organic chemistry, Angew. Chem. Int. Ed. 61 (2022) e202209539, https://doi.org/10.1002/anie.202209539.

[21] V.D. Nguyen, V.T. Nguyen, S. Jin, H.T. Dang, O.V. Larionov, Organoboron chemistry comes to light: recent advances in photoinduced synthetic approaches to organoboron compounds, Tetrahedron 75 (2019) 584–602, https://doi.org/10.1016/j.tet.2018.12.040.

[22] T. Ishiyama, M. Murata, N. Miyaura, Palladium(0)-Catalyzed cross-coupling reaction of alkoxydiboron with haloarenes: a direct procedure for arylboronic esters, J. Org. Chem. 60 (1995) 7508–7510, https://doi.org/10.1021/jo00128a024.

[23] C. Munteanu, T.E. Spiller, J. Qiu, A.J. DelMonte, S.R. Wisniewski, E.M. Simmons, D.E. Frantz, Pd- and Ni-based systems for the catalytic borylation of aryl (Pseudo) halides with $B_2(OH)_4$, J. Org. Chem. 85 (2020) 10334–10349, https://doi.org/10.1021/acs.joc.0c00929.

[24] W.K. Chow, O.Y. Yuen, P.Y. Choy, C.M. So, C.P. Lau, W.T. Wong, F.Y. Kwong, A decade advancement of transition metal-catalyzed borylation of aryl halides and sulfonates, RSC Adv. 3 (2013) 12518–12539, https://doi.org/10.1039/C3RA22905J.

[25] R.M. Fornwald, A. Yadav, J.R. Montero Bastidas, M.R. Smith, R.E. Maleczka, Simple and green preparation of tetraalkoxydiborons and diboron diolates from tetrahydroxydiboron, J. Org. Chem. 89 (2024) 6048–6052, https://doi.org/10.1021/acs.joc.3c02992.

[26] K. Arrington, G.A. Barcan, N.A. Calandra, G.A. Erickson, L. Li, L. Liu, M.G. Nilson, I.I. Strambeanu, K.F. VanGelder, J.L. Woodard, S. Xie, C.L. Allen, J.A. Kowalski, D. C. Leitch, Convergent synthesis of the NS5B inhibitor GSK8175 enabled by transition metal catalysis, J. Org. Chem. 84 (2019) 4680–4694, https://doi.org/10.1021/acs.joc.8b02269.

[27] O.T. Ring, A.D. Campbell, B.R. Hayter, L. Powell, Significant rate enhancement via potassium pivalate in a Miyaura borylation approach to verinurad, Tetrahedron Lett. 61 (2020) 151589, https://doi.org/10.1016/j.tetlet.2019.151589.

[28] S. Barroso, M. Joksch, P. Puylaert, S. Tin, S.J. Bell, L. Donnellan, S. Duguid, C. Muir, P. Zhao, V. Farina, D.N. Tran, J.G. de Vries, Improvement in the palladium-catalyzed Miyaura borylation reaction by optimization of the base: scope and mechanistic study, J. Org. Chem. 86 (2021) 103–109, https://doi.org/10.1021/acs.joc.0c01758.

[29] T.B. Boit, A.S. Bulger, J.E. Dander, N.K. Garg, Activation of C–O and C–N bonds using non-precious-metal catalysis, ACS Catal. 10 (2020) 12109–12126, https://doi.org/10.1021/acscatal.0c03334.

[30] T. Zhou, M. Szostak, Palladium-catalyzed cross-couplings by C–O bond activation, Catal. Sci. Technol. 10 (2020) 5702–5739, https://doi.org/10.1039/D0CY01159B.

[31] T. Ben Halima, W. Zhang, I. Yalaoui, X. Hong, Y.-F. Yang, K.N. Houk, S. G. Newman, Palladium-catalyzed Suzuki–Miyaura coupling of aryl esters, J. Am. Chem. Soc. 139 (2017) 1311–1318, https://doi.org/10.1021/jacs.6b12329.

[32] H. Kinuta, J. Hasegawa, M. Tobisu, N. Chatani, Rhodium-catalyzed borylation of aryl and alkenyl pivalates through the cleavage of carbon–oxygen bonds, Chem. Lett. 44 (2015) 366–368, https://doi.org/10.1246/cl.141084.

[33] H. Kinuta, M. Tobisu, N. Chatani, Rhodium-catalyzed borylation of aryl 2-pyridyl ethers through cleavage of the carbon–oxygen bond: borylative removal of the directing group, J. Am. Chem. Soc. 137 (2015) 1593–1600, https://doi.org/10.1021/ja511622e.

[34] R. Seki, N. Hara, T. Saito, Y. Nakao, Selective C–O bond reduction and borylation of aryl ethers catalyzed by a rhodium–aluminum heterobimetallic complex, J. Am. Chem. Soc. 143 (2021) 6388–6394, https://doi.org/10.1021/jacs.1c03038.

[35] K. Huang, D.-G. Yu, S.-F. Zheng, Z.-H. Wu, Z.-J. Shi, Borylation of aryl and alkenyl carbamates through Ni-catalyzed C–O activation, Chem. Eur J. 17 (2011) 786–791, https://doi.org/10.1002/chem.201001943.

[36] C. Zarate, R. Manzano, R. Martin, Ipso-borylation of aryl ethers via Ni-catalyzed C–OMe cleavage, J. Am. Chem. Soc. 137 (2015) 6754–6757, https://doi.org/10.1021/jacs.5b03955.

[37] K. Nakamura, M. Tobisu, N. Chatani, Nickel-catalyzed formal homocoupling of methoxyarenes for the synthesis of symmetrical biaryls via C–O bond cleavage, Org. Lett. 17 (2015) 6142–6145, https://doi.org/10.1021/acs.orglett.5b03151.

[38] M. Tobisu, J. Zhao, H. Kinuta, T. Furukawa, T. Igarashi, N. Chatani, Nickel-catalyzed borylation of aryl and benzyl 2-pyridyl ethers: a method for converting a robust ortho-directing group, Adv. Synth. Catal. 358 (2016) 2417–2421, https://doi.org/10.1002/adsc.201600336.

[39] W.L. Pein, E.M. Wiensch, J. Montgomery, Nickel-catalyzed ipso-borylation of silyloxyarenes via C–O bond activation, Org. Lett. 23 (2021) 4588–4592, https://doi.org/10.1021/acs.orglett.1c01280.

[40] X. Zeng, Y. Zhang, Z. Liu, S. Geng, Y. He, Z. Feng, Iron-catalyzed borylation of aryl ethers via cleavage of C–O bonds, Org. Lett. 22 (2020) 2950–2955, https://doi.org/10.1021/acs.orglett.0c00679.

[41] S. Geng, J. Zhang, S. Chen, Z. Liu, X. Zeng, Y. He, Z. Feng, Development and mechanistic studies of iron-catalyzed construction of Csp^2–B bonds via C–O bond activation, Org. Lett. 22 (2020) 5582–5588, https://doi.org/10.1021/acs.orglett.0c01937.

[42] J.M. Dennis, N.A. White, R.Y. Liu, S.L. Buchwald, Pd-catalyzed C–N coupling reactions facilitated by organic bases: mechanistic investigation leads to enhanced reactivity in the arylation of weakly binding amines, ACS Catal. 9 (2019) 3822–3830, https://doi.org/10.1021/acscatal.9b00981.

[43] R.S. Villatoro, J.R. Belfield, H.D. Arman, L.W. Hernandez, E.M. Simmons, Z. J. Garlets, S.R. Wisniewski, J.R. Coombs, D.E. Frantz, General method for Ni-catalyzed C–N cross-couplings of (Hetero)Aryl chlorides with anilines and aliphatic amines under homogeneous conditions using a dual-base strategy, Organometallics 42 (2023) 3164–3172, https://doi.org/10.1021/acs.organomet.3c00419.

[44] M.J. Goldfogel, X. Guo, J.L. Meléndez Matos, J.A. Gurak Jr., M.V. Joannou, W. B. Moffat, E.M. Simmons, S.R. Wisniewski, Advancing base-metal catalysis: development of a screening method for nickel-catalyzed Suzuki–Miyaura reactions of pharmaceutically relevant heterocycles, Org. Process Res. Dev. 26 (2022) 785–794, https://doi.org/10.1021/acs.oprd.1c00210.

[45] J. Becica, D.C. Leitch, C–O bond activation as a strategy in palladium-catalyzed cross-coupling, Synlett 32 (2021) 641–646, https://doi.org/10.1055/a-1306-3228.

[46] J. Becica, G. Gaube, W.A. Sabbers, D.C. Leitch, Oxidative addition of activated aryl-carboxylates to Pd(0): divergent reactivity dependant on temperature and structure, Dalton Trans. 49 (2020) 16067–16071, https://doi.org/10.1039/D0DT01119C.

[47] J. Becica, O.R.J. Heath, C.H.M. Zheng, D.C. Leitch, Palladium-catalyzed cross-coupling of alkenyl carboxylates, Angew. Chem. Int. Ed. 59 (2020) 17277–17281, https://doi.org/10.1002/anie.202006586.

[48] N. Pipaón Fernández, G. Gaube, K.J. Woelk, M. Burns, D.P. Hruszkewycz, D. C. Leitch, Palladium-catalyzed direct C–H alkenylation with enol pivalates proceeds via reversible C–O oxidative addition to Pd(0), ACS Catal. 12 (2022) 6997–7003, https://doi.org/10.1021/acscatal.2c01305.

[49] G. Gaube, N. Pipaon Fernandez, D.C. Leitch, An evaluation of palladium-based catalysts for the base-free borylation of alkenyl carboxylates, New J. Chem. 45 (2021) 20095–20098, https://doi.org/10.1039/D1NJ04008A.
[50] J. Huang, M. Isaac, R. Watt, J. Becica, E. Dennis, M.I. Saidaminov, W.A. Sabbers, D. C. Leitch, DMPDAB–Pd–MAH: a versatile Pd(0) source for precatalyst formation, reaction screening, and preparative-scale synthesis, ACS Catal. 11 (2021) 5636–5646, https://doi.org/10.1021/acscatal.1c00288.
[51] N. Oka, T. Yamada, H. Sajiki, S. Akai, T. Ikawa, Aryl boronic esters are stable on silica gel and reactive under Suzuki–Miyaura coupling conditions, Org. Lett. 24 (2022) 3510–3514, https://doi.org/10.1021/acs.orglett.2c01174.
[52] S.E. Shockley, J.C. Holder, B.M. Stoltz, Palladium-catalyzed asymmetric conjugate addition of arylboronic acids to α,β-unsaturated cyclic electrophiles, Org. Process Res. Dev. 19 (2015) 974–981, https://doi.org/10.1021/acs.oprd.5b00169.
[53] A.-L. Lee, Enantioselective oxidative boron Heck reactions, Org. Biomol. Chem. 14 (2016) 5357–5366, https://doi.org/10.1039/C5OB01984B.
[54] X. Zhao, D. Zhang, X. Wang, Unraveling the mechanism of palladium-catalyzed base-free cross-coupling of vinyl carboxylates: dual role of arylboronic acids as a reducing agent and a coupling partner, ACS Catal. 12 (2022) 1809–1817, https://doi.org/10.1021/acscatal.1c00247.
[55] C.S. Wei, G.H.M. Davies, O. Soltani, J. Albrecht, Q. Gao, C. Pathirana, Y. Hsiao, S. Tummala, M.D. Eastgate, The impact of palladium(II) reduction pathways on the structure and activity of palladium(0) catalysts, Angew. Chem. Int. Ed. 52 (2013) 5822–5826, https://doi.org/10.1002/anie.201210252.
[56] Q. Liu, Synthesis of alkylboronic esters from alkyl iodides, Org. Synth. 99 (2022) 15–28, https://doi.org/10.15227/orgsyn.099.0015.
[57] J. Lu, S. Donnecke, I. Paci, D.C. Leitch, A reactivity model for oxidative addition to palladium enables quantitative predictions for catalytic cross-coupling reactions, Chem. Sci. 13 (2022) 3477–3488, https://doi.org/10.1039/D2SC00174H.
[58] J. Lu, H. Celuszak, I. Paci, D.C. Leitch, Quantitative reactivity models for oxidative addition to L2Pd(0): additional substrate classes, solvents, and mechanistic insights, Chem. Eur J. 30 (2024) e202402282, https://doi.org/10.1002/chem.202402282.
[59] N. Pipaón Fernández, O. Cruise, S.E.F. Easton, J.M. Kaplan, J.L. Woodard, D. P. Hruszkewycz, D.C. Leitch, Direct heterocycle C–H alkenylation via dual catalysis using a palladacycle precatalyst: multifactor optimization and scope exploration enabled by high-throughput experimentation, J. Org. Chem. (2024), https://doi.org/10.1021/acs.joc.3c02311.
[60] H.L.D. Hayes, R. Wei, M. Assante, K.J. Geogheghan, N. Jin, S. Tomasi, G. Noonan, A.G. Leach, G.C. Lloyd-Jones, Protodeboronation of (Hetero)Arylboronic esters: direct versus prehydrolytic pathways and self-/auto-catalysis, J. Am. Chem. Soc. 143 (2021) 14814–14826, https://doi.org/10.1021/jacs.1c06863.
[61] D.S. Matteson, Functional group compatibilities in boronic ester chemistry, J. Organomet. Chem. 581 (1999) 51–65, https://doi.org/10.1016/S0022-328X(99)00064-9.
[62] C.D. Roy, H.C. Brown, Stability of boronic esters – structural effects on the relative rates of transesterification of 2-(phenyl)-1,3,2-dioxaborolane, J. Organomet. Chem. 692 (2007) 784–790, https://doi.org/10.1016/j.jorganchem.2006.10.013.
[63] A. García-Domínguez, A.G. Leach, G.C. Lloyd-Jones, *In situ* studies of arylboronic acids/esters and R_3SiCF_3 reagents: kinetics, speciation, and dysfunction at the carbanion–ate interface, Acc. Chem. Res. 55 (2022) 1324–1336, https://doi.org/10.1021/acs.accounts.2c00113.
[64] V.K. Ahluwalia, C. Prakash, R. Gupta, A facile synthesis of 3-allylcoumarins, Synthesis 1980 (1980), https://doi.org/10.1055/s-1980-28920, 48–50.
[65] R.N. Bream, H. Clark, D. Edney, A. Harsanyi, J. Hayler, A. Ironmonger, N. Mc Cleary, N. Phillips, C. Priestley, A. Roberts, P. Rushworth, P. Szeto, M.R. Webb, K. Wheelhouse, Application of C–H functionalization in the development of a concise and convergent route to the phosphatidylinositol-3-kinase delta inhibitor nemiralisib, Org. Process Res. Dev. 25 (2021) 529–540, https://doi.org/10.1021/acs.oprd.0c00486.
[66] J. Caruano, G.G. Muccioli, R. Robiette, Biologically active γ-lactams: synthesis and natural sources, Org. Biomol. Chem. 14 (2016) 10134–10156, https://doi.org/10.1039/C6OB01349J.
[67] S. Chatterjee, R. Sahoo, S. Nanda, Recent reports on the synthesis of γ-butenolide, γ-alkylidenebutenolide frameworks, and related natural products, Org. Biomol. Chem. 19 (2021) 7298–7332, https://doi.org/10.1039/D1OB00875G.
[68] B. Rattray, D.J. Nugent, G. Young, Rofecoxib as adjunctive therapy for haemophilic arthropathy, Haemophilia 11 (2005) 240–244, https://doi.org/10.1111/j.1365-2516.2005.01087.x.
[69] J. Xie, S. Xue, E.C. Escudero-Adán, A.W. Kleij, Domino synthesis of α,β-unsaturated γ-lactams by stereoselective amination of α-tertiary allylic alcohols, Angew. Chem. Int. Ed. 57 (2018) 16727–16731, https://doi.org/10.1002/anie.201810160.
[70] S. Aubert, T. Katsina, S. Arseniyadis, A sequential Pd-AAA/Cross-Metathesis/Cope rearrangement strategy for the stereoselective synthesis of chiral butenolides, Org. Lett. 21 (2019) 2231–2235, https://doi.org/10.1021/acs.orglett.9b00521.
[71] J. Yan, W. Zhang, Q. He, J. Hou, H. Zeng, H. Wei, W. Xie, Enantioselective direct vinylogous Michael addition for constructing enantioenriched γ,γ-dialkyl substituted butyrolactams and octahydroindoles, Org. Biomol. Chem. 20 (2022) 2387–2391, https://doi.org/10.1039/D2OB00112H.